Journal of Research and Applications in Mechanical Engineering
ISSN: 2229-2152 (Print); 2697-424x (Online)
(2025) Vol. 13, No. 1, Paper No. JRAME-25-13-015
[DOI: 10.14456/jrame.2025.15]

Research Article

Influence of Inserted Different Ribs Configuration in 2D Horizontal Channel on Characteristics Turbulent Fluid Flow and Forced Heat Transfer: A Numerical Investigation

S.A. Ali*
Department of Automobile Engineering, College of Engineering -Al Musayab, University of Babylon, Iraq

Received 2 August 2024
Revised 17 September 2024
Accepted 4 October 2024

Abstract:
The current study deals with the analysis of a two-dimensional (2D) single-phase turbulent airflow in a channel having ribs of different configurations. COMSOL Multiphysics software was used to investigate all cases that were carried out numerically using the standard k-ε model. Several parameters were studied as a variable function against the Reynolds number in ranges (9000 to 18000), including the rate of heat transfer, friction factor, and pressure difference of all rib shapes compared to the empty channel. The shape plays an important role in the characteristics of fluid flow and heat transfer distribution and the circular rib shows better heat transfer performance and friction factor compared to the normal channel and other designs, therefore, the circular design ensures improved thermal-hydraulic performance. Also, the percentage of increase in the heat transfer rate represented by Nusselt number (71.48, 69.99, and 67.29%) for rib designs (quarter circle, square, and triangle) respectively compared to the channel without ribs. As the Reynolds number rises, the pressure drop across the fluid entry-exit zone of the channel is influenced by the ribs being inserted inside as well as when the channel is empty.

Keywords: *Turbulent fluid flow, Heat transfer, Ribs, 2D Channel, Pressure drop*

1. Introduction

Due to the development of the thermal boundary layer, the thermal performance is generally poor in most conventional heat exchanger systems, which causes a low coefficient of convective heat transfer between the heated surface of the system and the working media. To enhance convective heat transfer and reduce the overall thermal resistance, a thinner thermal boundary layer is required in the heated surface of the heat exchanger system, which leads to energy savings and a smaller heat exchanger size. Vortex flow or obstruction devices are used in engineering and industrial applications on a large scale to improve the heat transfer process. Where the vortex generators and the disruption of the boundary layer affect the enhancement of the coefficient of convective heat transfer and momentum transfer, as in pipes and channels such as; fins [1, 2], ribs [3, 4], baffles [5-7], wire coil [8, 9], twisted tapes [10-13], and wing-lets [14-17]. Many researchers have studied in their research papers the effect of generating vortices and blocking the flow of fluids to further improve heat transfer rate and one of these methods is the use of ribs.

* Corresponding author: S.A. Ali
E-mail address: sarmad.ahmed96@uobabylon.edu.iq

Lu et al. [18] presented an experimental and numerical study that deals with the introduction of longitudinal vortex generators into the gaps of three-dimensional stacked chips to enhance heat transfer. Depending on the mass flow rate and heating power, as well as the spacing of the longitudinal vortex generators, experimental and numerical tests were performed on the performance of a three-dimensional stacked chip with and without longitudinal vortex generators in the gap. Numerical and experimental results have shown that the longitudinal vortex generator set can effectively improve the cooling performance of the chip with a small gap. Zhao et al. [19] performed a numerical study looking to enhance the overall performance of the fin tube heat exchanger by arranging a new combination of curved, rectangular, and straight-wing vortex generator pairs into a common flow configuration. To simplify the flow, temperature distribution, and pressure field, the effects of the rectangular wing vortex generator were compared with those of the non-rectangular wing vortex generator, and then the thermo-hydraulic performance and overall performance were numerically investigated between cases with different locations and sizes of the rectangular wing vortex generator. Skullong et al. [20] presented an experimental study dealing with the properties of thermal resistance and flow in a tubular heat exchanger equipped with wing-overlapping perforated tapes. The check tube has a constant wall heat flux for turbulent airflow in the Reynolds number range (4180-26000). The use of perforated wing tapes to generate longitudinal vortex flows disrupts the thermal boundary layer on the pipe wall and provides a stronger mixing of liquids. Sinha et al. [21] researched a numerical study that simulates the airflow in fin-tube type heat exchangers with half the height of the duct as vortex generators acting as a pair of rectangular wings. The heat exchanger is rounded as a periodic rectangular channel with heated walls and three rows of built-in pipes located at a specified interval. The first is for three tubular rows and the second is a staggered arrangement of three tubular rows with a variety of angles of attack in all directions. Ohta et al. [22] presented a numerical study that simulates laminar boundary layer flow to enhance heat transfer in a flat plate with arrays of tetrahedral vortex generators. When the prevailing angle is equal to 60 degrees, the Nusselt number is closely related to the prevailing angle. The parallax caused by a pair of vortices is revealed based on the analysis of each term of an energy equation with an average Reynolds number as the dominant factor the value of the detente angle is equal to zero. Using a turbulent component with an increase in the prevailing angle the heat transfer is enhanced. Aridi et al. [23] displayed a numerical study looking for a new design that combines a multi-drain water application with a high-efficiency vortex generator-based heat exchanger. Several operational parameters have been studied, including the investigation of the effect of heat transfer, flow rate, total heat transfer as well as thermal reinforcement. Four different types of input energy were studied, including diesel, gas, electricity, and coal. Besides the investigation of the sustainability of the system, the economic and environmental impacts were studied. Elwekeel et al. [24] displayed a numerical study of turbulent flow in a channel with a rectangular cross-section. The lower wall of the channel is exposed to a heat flow condition while the upper wall is insulated. Several coefficients have been studied including the investigation of forced load, flow friction, and the horizontal air performance factor. Different types of ribs were used inside the rectangular channel to generate vortices to increase the heat transfer process, square-triangular-trapezoidal ones for the Reynolds number range (8000 - 20000).

The current numerical turbulent airflow simulation uses the commercial CFD program (COMSOL Multiphysics) to study the effect of inserting different shapes of ribs inside a 2D horizontal channel exposed to a constant heat flux of (18 $kW.m^{-2}$) on the bottom wall and insulation from the top on enhance heat transfer process (represent by Nusselt number) thus improve the performance and efficiency of the gas turbine blade and heat exchanger as one of the common engineering industrial applications of this study. The research gap of the current study compared to the previous literature was the use of different rib designs with different extents of the Reynolds number.

2. Computational Information of Present Work

The current modeling investigates the distribution of heat transfer in a ribbed two-dimensional channel and the steady state, turbulent flow field using the conventional k-ε turbulence model. COMSOL, version 6.0, is the simulation program used for the computational analysis. The finite element approach is used by COMSOL Multiphysics to solve the fluid flow and heat transfer governing equations. An appropriate turbulence model is therefore required for simulations to forecast the flow field and temperature distribution with any degree of accuracy. Previous research has demonstrated that the k-ε model can accurately predict the flow characteristics at the back of the ribs and in the bend of channels. Additionally, it has been found that the k-ε model's conclusions for heat transmission and pressure loss in channels closely match experimental findings. Therefore, the typical k-ε model was used for the present investigation to determine the features of pressure drop and transfer of heat (Nusselt number).

2.1 Explanation of the Computational Model

The domain of the computational model utilized for the simulation is shown in Fig. 1. The geometry's dimensions are all expressed in meters. All rib geometries are included in the current computational investigation, as shown in Fig. 2. However, Figs. 1 and 3 only display the geometry and mesh of square ribs. The only differences between the four studied ribs' geometries are their respective cross-sectional areas. The test section's height (H of 0.08 m) and its length (L of 0.55 m). For every summary of instances examined, only the bottom wall was subjected heat flux of (18000 W/m^2) while the top wall was thermally insulation. The pressure-correction system, which separates the energy and momentum equations, is used in the parametric separated solver used in this simulation. To create the pressure and velocity connection, a simplified approach was employed. Previous studies showed that the heat transfer and fluid flow characteristics in a channel may be correctly predicted using Reynolds of Average Navier -Stokes (RANS) models.

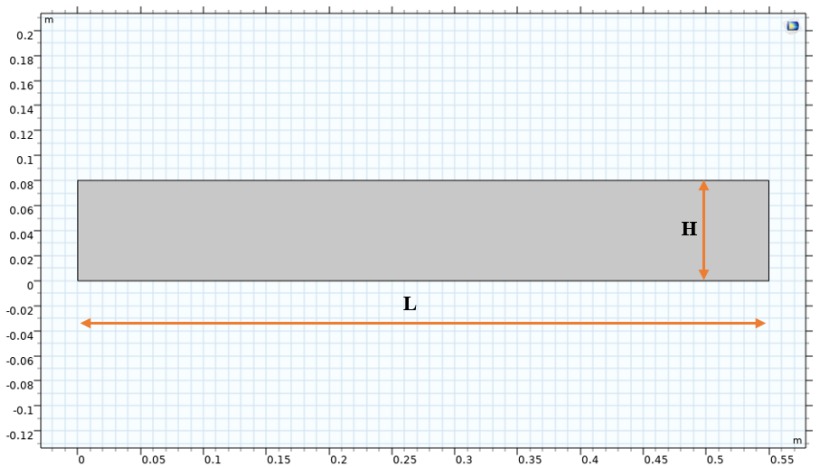

Fig. 1. Test section of the computational domain.

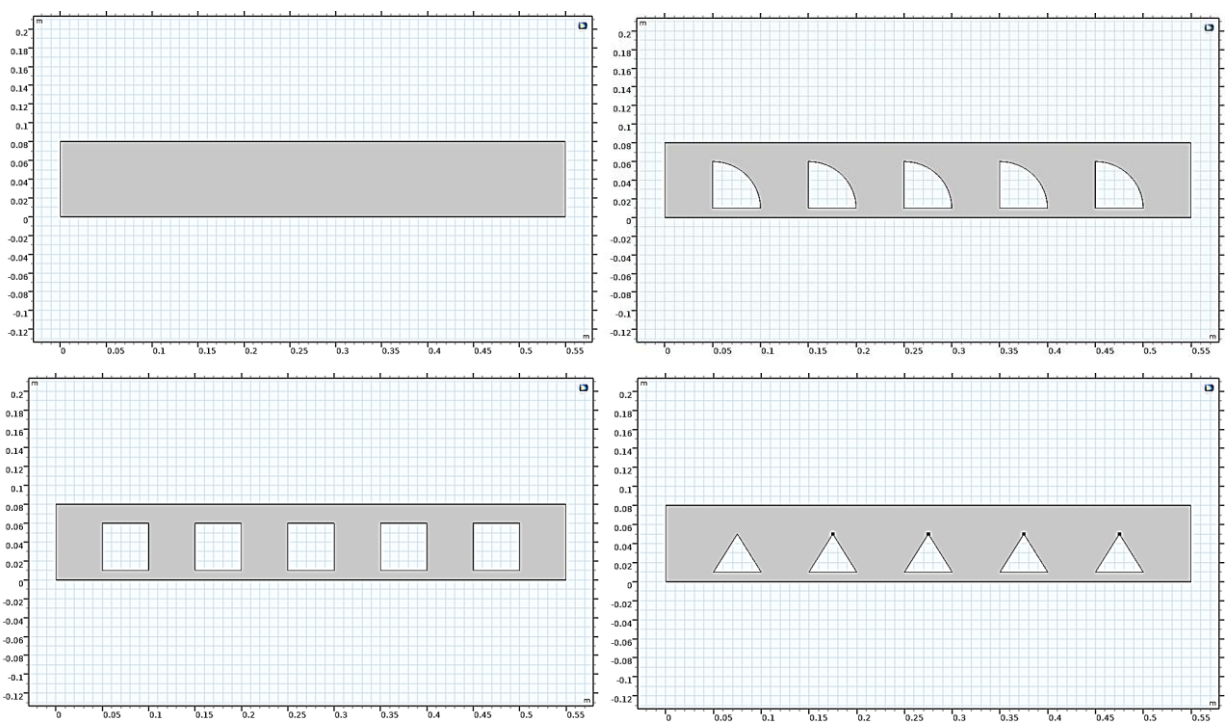

Fig. 2. Configurations of the geometry ribs that were employed in this study.

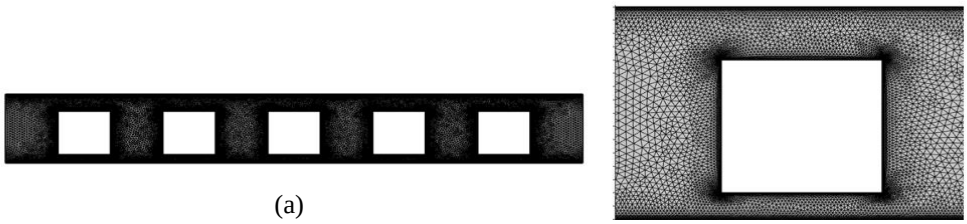

(a) (b)

Fig. 3. (a) General view mesh of the computational domain and (b) Cut for a mesh section of a square rib.

2.2 Governing Equations

Due to the minor temperature change along the channel length, air is considered an incompressible fluid with constant physical characteristics in this study. Below is an expression of the standard governing fluid flow equations for various variables. Considering that the current study makes use of conductive and convective heat equations in the air and the solid wall, as well as constant Reynolds averaged Navier-Stokes (RANS) equations in the air domain. Fluid-thermal interaction modeling is made simple by the preset Multiphysics coupling of turbulent non-isothermal flow, which sets up these application modes and application couplings [25]:

Equation of Continuity:

$$\frac{\partial}{\partial x_i}(\rho u_i) = 0 \tag{1}$$

Equation of Momentum:

$$\frac{\partial}{\partial x_i}(\rho u_j u_i) = -\frac{\partial p}{\partial x_i} + \frac{\partial}{\partial x_j}[\mu(\frac{\partial u_i}{\partial x_j} + \frac{\partial u_j}{\partial x_i})] + \frac{\partial}{\partial x_j}(-\rho \overline{u_i' u_j'}) \tag{2}$$

Equation of heat Energy:

$$\frac{\partial}{\partial x_i}(\rho u_j T) = \frac{\partial}{\partial x_j}((\frac{\mu}{\Pr} + \frac{\mu_t}{\Pr_t})\frac{\partial T}{\partial x_j}) \tag{3}$$

2.3 Boundary Conditions

Under ambient conditions and with constant characteristics, incompressible air was chosen as the working fluid. The flow type is turbulent, non-rotating, and with a constant two-dimensional flow. The velocity of the fluid at the entrance to the channel was determined by the specified Reynolds number with temperature uniformity from the entrance (300K). The lower surface of the channel is exposed to a constant uniform heat flux (18000 W / m^2). All walls of the channel are superimposed at constant temperature and have impermeable no-slip for velocity. All boundary conditions applied in channel simulation tests are summarized in Table 1. Also, Table 2 shows the thermophysical properties of the working fluid inside the channel.

Table 1: Summary of boundary conditions applicable to all simulation tests.

Operation Parameter	**Boundary Condition**
Inlet	Velocity inlet
Outlet	Outlet pressure
Fluid inlet temperature	300K
Bottom wall channel	Heat Flux of 18000 W/m^2
Top wall channel	Thermal Insulation
Re	9000 to 18000

Table 2: Thermophysical properties of the working fluid (Air) at a temperature of (300K).

Properties	Unit	Value
Specific heat capacity	kJ/kg. K	1.0057
Thermal conductivity	W/m. K	0.0626
Dynamic viscosity	Pa. s	0.0000184
Density	Kg/m^3	1.177

3. Study of Grid Independence

Fig. (4) provides an investigation of the grid independence of the computational domain to ensure that the results obtained are independent of the size of the grid. The grid independence of a channel without ribs was studied at the value of the Reynolds number (9000) by taking different types of mesh to divide the model into many elements. The results of the flow variance of the Nusselt number were compared against the number of elements obtained by choosing the type of grid independence.

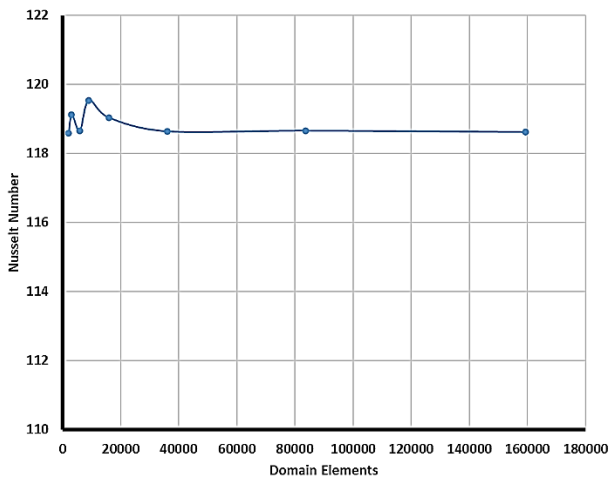

Fig. 4. Test of grid independence for the computational channel.

4. Computational Outcomes

4.1 Distribution of Temperatures

Fig. (5) presents the temperature distribution of the fluid flow (air) inside the channel with and without ribs at the value of the Reynolds number (9000). The temperature can be observed gradually increasing towards the flow axis. Using ribs, the temperature rate decreases compared to the empty channel due to the occupancy of the surface area. The percentage decrease of air temperature compared against the smooth channel (38.38, 34.49, and 33.64%) for different shapes of ribs (quarter circle, square, and triangle) respectively.

4.2 Distribution of Velocity

Fig. (6) shows the distribution of the velocity of the working fluid (air) inside the channel with and without ribs at the value of the Reynolds number (9000). The velocity can be observed as high as possible in the middle and decreases at the wall. With the use of ribs, the air velocity rate increases compared to the normal channel due to the obstruction of the flow and the presence of sharp angles of the ribs. The ratio of fluid velocity increased compared against the empty channel (76.26, 74.22, and 66.66 %) for different shapes of ribs (quarter circle, square, and triangle) respectively.

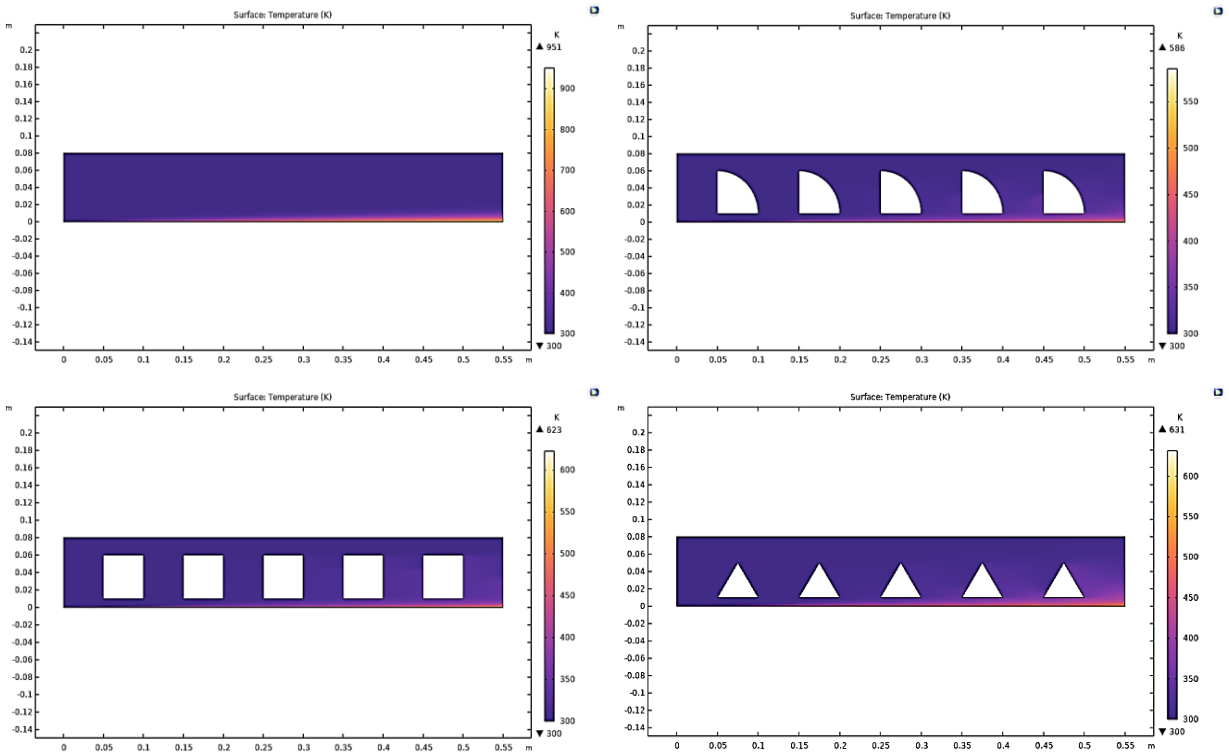

Fig. 5. Temperature distribution of a 2D channel for different shapes of ribs at Reynolds number of (9000).

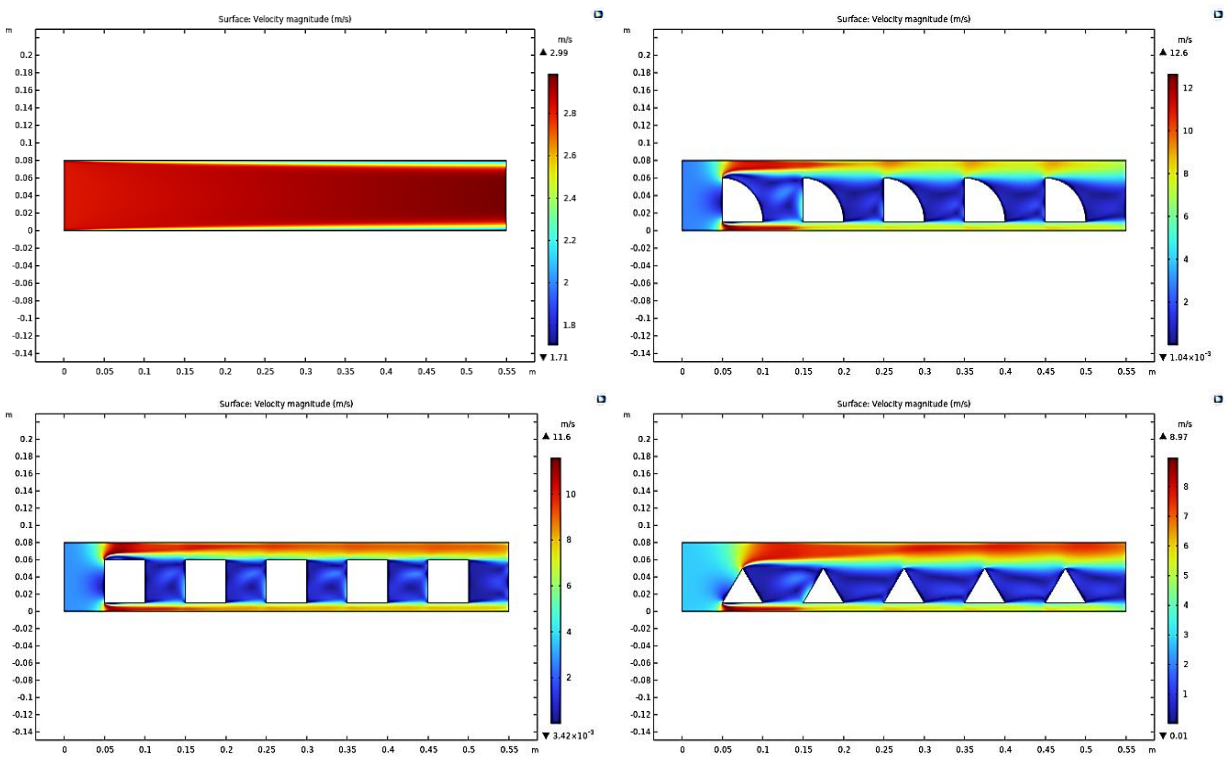

Fig. 6. Temperature distribution of a 2D channel for kinds shapes of ribs at Reynolds of (9000).

4.3 Distribution of Streamline

Fig. (7) shows the streamlines of the fluid with the constant heat flux and the Reynolds value at (9000) around the three ribs compared to the empty channel. A gradual decrease in fluidity can be observed towards the flow axis of the fluid, so the vortices are large at the front of the channel. Also, the quarter-circle rib was found to produce very large separation bubbles directly behind the rib, a likely cause of which is the upward flow due to the sloping front surface of the rib.

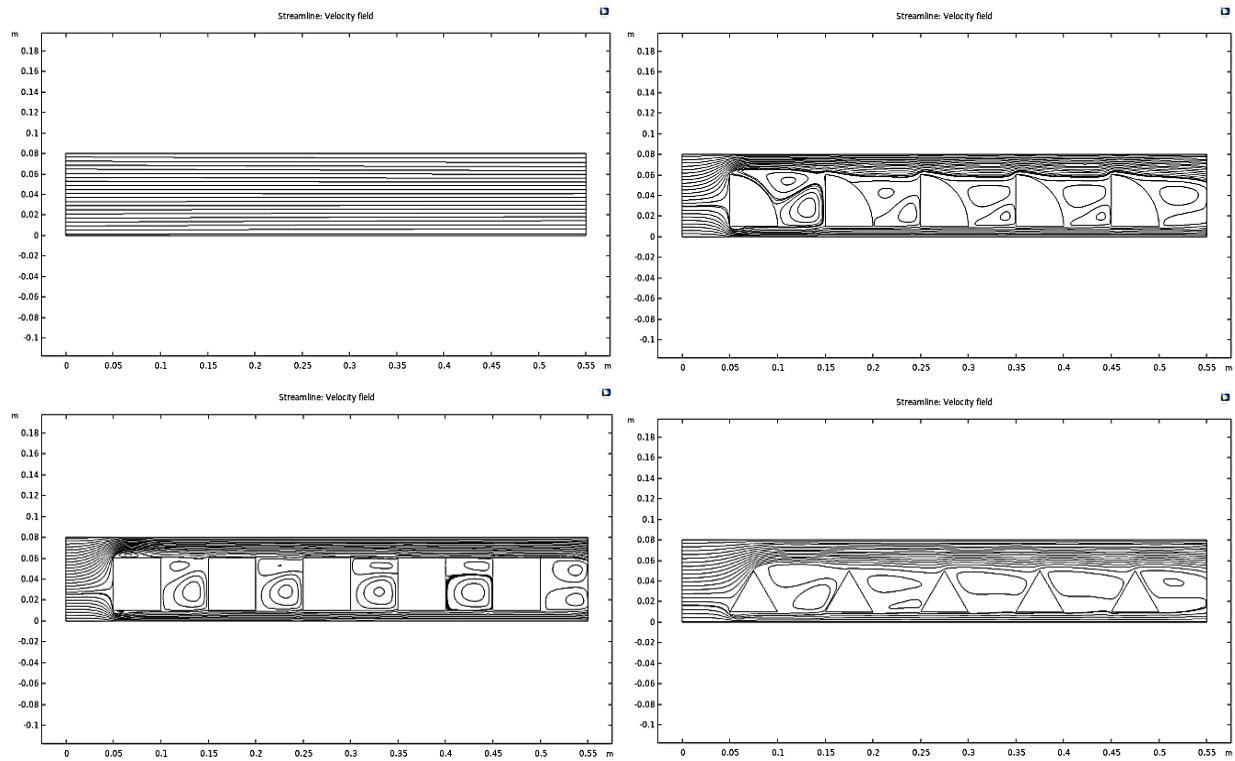

Fig. 7. Streamline distribution of 2D channel for different shapes of ribs at Reynolds number of (9000).

4.4 Distribution of Pressure

Fig. (8) deals with the distribution of the pressure rate of the empty channel surface against the use of ribs to improve heat transfer. The pressure rate can be observed to increase significantly when the rib is placed inside the empty channel. The quarter rib of the circle gave the highest average pressure values of the other ribs (square and triangle) compared to the normal channel with an increase of (98.95, 98.82, and 98%), respectively.

4.5 Nusselt Number

Fig. (9) presents the distribution of the forced convection heat transfer rate represented by the Nusselt number against the Reynolds number with different ranges (9000-18000). It can be observed that the number of Nusselt increases gradually as the fluid velocity increases during the flow and also increases with the use of ribs compared to the empty channel. The ratio of the increase of the Nusselt number for the three various ribs (quarter circle, square, triangle) is (71.48, 69.99, and 67.29%) respectively.

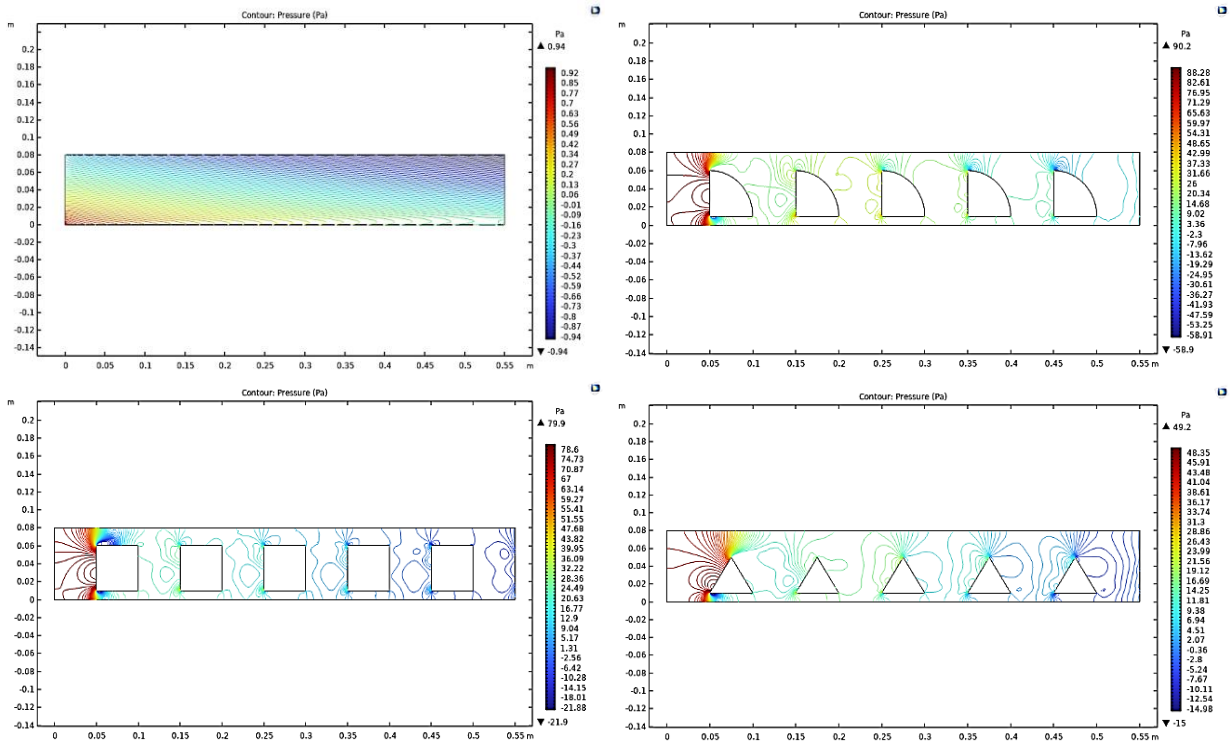

Fig. 8. Contour pressure distribution of 2D channel for different shapes of ribs at Reynolds number of (9000).

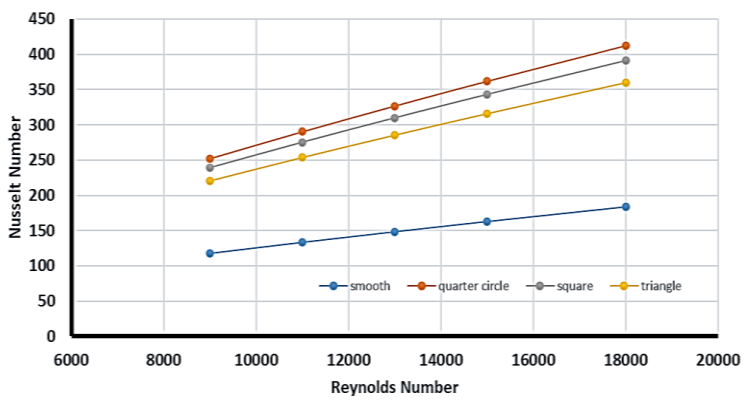

Fig. 9. Variation of Nusselt number with Reynolds number for different configurations of channel.

4.6 Pressure Drop and Friction Factor

Fig. (10) shows the change of the pressure difference across the inlet and outlet of the channel and also the change of the friction factor against the Reynolds number. The observed velocity of the fluid can be caused by an increase in the amount of pressure. The shape of the ribs also affects the pressure change compared to the channel without ribs. The friction factor decreases gradually by increasing the fluid velocity and by changing the shapes of the ribs as a result of the velocity inversely proportional to the friction factor.

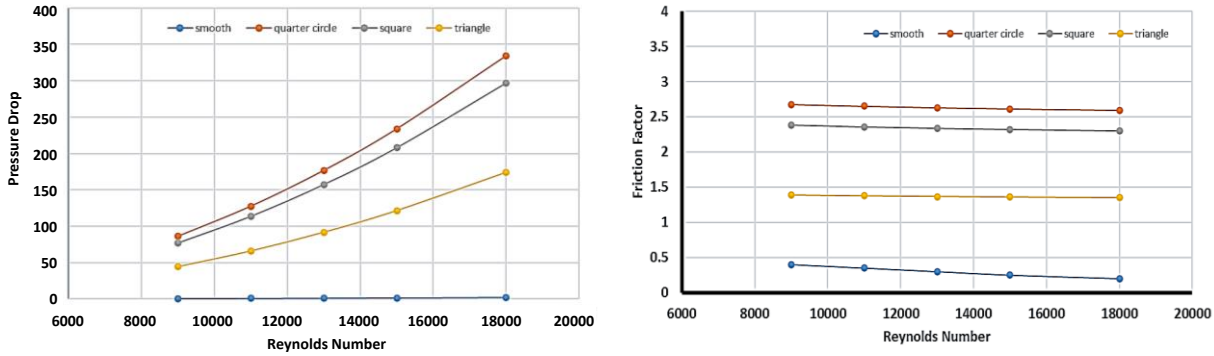

Fig. 10. Variation of pressure drop and friction factor with Reynolds number for different configurations of channel.

5. Conclusions

Numerical analysis of computational fluid dynamics using the COMSOL Multiphysics program to improve the heat transfer process and airflow characteristics of a 2D channel with height and length of (0.08 and 0.55 m) respectively using ribs of different shapes (quarter circle, square, and triangle) to focus on the optimal design of the rib to improve thermal performance. The numerical simulation result deduced several points as follows:

1) The characteristics of the fluid flow and heat transfer of the channel are influenced by the presence of ribs.
2) The design of the circular rib improves heat transfer compared to other designs (quarter circular-Square) and also the normal channel.
3) The primary finding from the computational analysis above is that crucial parameters related to heat transfer and fluid flow across the ribbed surface of a channel can be computed using Reynolds-averaged Navier-Stokes-based equations and a suitable turbulence model.
4) The quarter circle rib provided the highest heat transfer performance for the Reynolds number under consideration, with a pressure loss performance higher than the other ribs, while the smooth channel provided the best pressure loss performance.
5) The rib design plays a very important role in determining the heat transfer rate, the design with more bends has a higher heat transfer rate.
6) In general, the coefficient of heat transfer by forced convection gradually improves with increasing fluid velocity (Reynolds number).
7) The percentage of increase in the heat transfer rate is represented by the Nusselt number (71.48, 69.99, and 67.29%) for rib designs (quarter circle, square, and triangle) respectively compared to the channel without ribs.
8) The pressure drop across the fluid entry-exit zone of the channel is affected by the inserting of ribs inside as well compared to the empty channel gradually increases with an increase in the Reynolds number.

Nomenclature

H	Height of channel, m
k	Kinetic of turbulence heat energy
L	Length of channel, m
p	Fluid pressure, $N.m^{-2}$
Pr	Prandtl Number
Re	Reynolds number
T	Fluid temperature, K
u	Velocity of fluid, $m.s^{-1}$

Greek symbols

μ	Fluid dynamic viscosity, Ns/m^2
μ_t	Turbulent dynamic viscosity, Ns/m^2
ε	Kinetic dissipation of turbulence heat energy
ρ	Fluid density, kg/m^3

Abbreviations

2D	Two Dimensional
CFD	Computational Fluid Dynamics
COMSOL	Computer Solution
RANS	Reynolds of Average Navier -Stokes

References

[1] Promvonge P, Skullong S, Kwankaomeng S, Thiangpong C. Heat transfer in square duct fitted diagonally with angle-finned tape—part 1: experimental study. Int Commun Heat Mass Transf. 2012;39(5):617-624.

[2] Promvonge P, Skullong S, Kwankaomeng S, Thiangpong C. Heat transfer in square duct fitted diagonally with angle-finned tape—part 2: numerical study. Int Commun Heat Mass Transf. 2012;39(5):625-633.

[3] Thianpong C, Chompookham T, Skullong S, Promvonge P. Thermal characterization of turbulent flow in a channel with isosceles triangular ribs. Int Commun Heat Mass Transf. 2009;36(7):712-717.

[4] Skullong S, Kwankaomeng S, Thianpong C, Promvonge P. Thermal performance of turbulent flow in a solar air heater channel with rib-groove turbulators. Int Commun Heat Mass Transf. 2014;50:34-43.

[5] Promvonge P, Sripattanapipat S, Kwankaomeng S. Laminar periodic flow and heat transfer in square channel with 45 inline baffles on two opposite walls. Int J Therm Sci. 2010;49(6):963-975.

[6] Sriromreun P, Thianpong C, Promvonge P. Experimental and numerical study on heat transfer enhancement in a channel with Z-shaped baffles. Int Commun Heat Mass Transf. 2012;39(7):945-952.

[7] Tamna S, Skullong S, Thianpong C, Promvonge P. Heat transfer behaviors in a solar air heater channel with multiple V-baffle vortex generators. Sol Energy. 2014;110:720-735.

[8] Promvonge P. Thermal performance in circular tube fitted with coiled square wires. Energy Convers Manage. 2008;49(5):980-987.

[9] Chang SW, Gao JY, Shih HL. Thermal performances of turbulent tubular flows enhanced by ribbed and grooved wire coils. Int J Heat Mass Transf. 2015;90:1109-1124.

[10] Eiamsa-Ard S, Thianpong C, Promvonge P. Experimental investigation of heat transfer and flow friction in a circular tube fitted with regularly spaced twisted tape elements. Int Commun Heat Mass Transf. 2006;33(10):1225-1233.

[11] Eiamsa-Ard S, Promvonge P. Performance assessment in a heat exchanger tube with alternate clockwise and counter-clockwise twisted-tape inserts. Int J Heat Mass Transf. 2010;53(7-8):1364-1372.

[12] Chang SW, Guo MH. Thermal performances of enhanced smooth and spiky twisted tapes for laminar and turbulent tubular flows. Int J Heat Mass Transf. 2012;55(25-26):7651-7667.

[13] Chokphoemphun S, Pimsarn M, Thianpong C, Promvonge P. Thermal performance of tubular heat exchanger with multiple twisted-tape inserts. Chin J Chem Eng. 2015;23(5):755-762.

[14] Min C, Qi C, Wang E, Tian L, Qin Y. Numerical investigation of turbulent flow and heat transfer in a channel with novel longitudinal vortex generators. Int J Heat Mass Transf. 2012;55(23-24):7268-7277.

[15] Zhou G, Ye Q. Experimental investigations of thermal and flow characteristics of curved trapezoidal winglet type vortex generators. Appl Therm Eng. 2012;37:241-248.

[16] Zhou G, Feng Z. Experimental investigations of heat transfer enhancement by plane and curved winglet type vortex generators with punched holes. Int J Therm Sci. 2014;78:26-35.

[17] Chokphoemphun S, Pimsarn M, Thianpong C, Promvonge P. Heat transfer augmentation in a circular tube with winglet vortex generators. Chin J Chem Eng. 2015;23(4):605-614.

[18] Lu Z, Li M, Yang C, Cheng X, Zhang J. Experimental and numerical study on the heat transfer and flow characteristics of micro-gap chip with longitudinal vortex generator array. Case Stud Therm Eng. 2023;45:102979.

[19] Zhao L, Qian Z, Wang X, Wang Q, Li C, Zhang Z. Analysis of the thermal improvement of plate fin-tube heat exchanger with straight and curved rectangular winglet vortex generators. Case Stud Therm Eng. 2023;51:103612.

[20] Skullong S, Promvonge P, Thianpong C, Pimsarn M. Heat transfer and turbulent flow friction in a round tube with staggered-winglet perforated-tapes. Int J Heat Mass Transf. 2016;95:230-242.

[21] Sinha A, Chattopadhyay H, Iyengar AK, Biswas G. Enhancement of heat transfer in a fin-tube heat exchanger using rectangular winglet type vortex generators. Int J Heat Mass Transf. 2016;101:667-681.

[22] Ohta T, Mitsuishi A, Shimura T, Iwamoto K, Murata A. Dependence of mainstream angle of vortex generator arrays on heat transfer enhancement in boundary layer flow on flat plate based on direct numerical simulation. Int J Heat Mass Transf. 2022;198:123362.

[23] Aridi R, Ali S, Lemenand T, Faraj J, Khaled M. Innovative concept of vortex generator-equipped multi-drain heat recovery systems–numerical study and energetic analysis. Int J Thermofluids. 2023;20:100455.
[24] Elwekeel FN, Zheng Q, Abdala AM. Air/mist cooling in a rectangular duct with varying shapes of ribs. Proc Inst Mech Eng C: J Mech Eng Sci. 2014;228(11):1925-1935.
[25] Gawande VB, Dhoble AS, Zodpe DB, Chamoli S. Experimental and CFD investigation of convection heat transfer in solar air heater with reverse L-shaped ribs. Sol Energy. 2016;131:275-295.